

# Chaos and Diffusion in Dynamical Systems Through Stable-Unstable Manifolds

Massimiliano Guzzo

**Abstract** The phase-space structure of conservative non-integrable dynamical systems is characterized by a mixture of stable invariant sets and unstable structures which possibly support diffusion. In these situation, many practical and theoretical questions are related to the problem of finding orbits which connect the neighbourhoods of two points  $A$  and  $B$  of the phase-space. Hyperbolic dynamics has provided in the last decades many tools to tackle the problem related to the existence and the properties of the so called stable and unstable manifolds, which provide natural paths for the diffusion of orbits in the phase-space. In this article we review some basic results of hyperbolic dynamics, through the analysis of the stable and unstable manifolds in basic mathematical models, such as the symplectic standard map, up to more complicate models related to the Arnold diffusion.

## 1 Introduction

Diffusion in conservative dynamical systems has been intensively studied in the last decades by means of analytical and numerical techniques. The problem is particularly complicate and interesting for non-integrable systems, because the phase-space is filled by a mixture of stable invariant sets and structures of peculiar topology which possibly support diffusion. The most famous example of non-integrable system is represented by the three body problem, which has motivated most of the researches done in this field. Many branches of dynamical systems theory, such as the KAM theory, hyperbolic theory, numerical investigations of dynamical systems with dynamical indicators, have been developed and tested on gravitational problems, such as the classical three body problem and the stability problems in our Solar System, up to the more recent problems related to space flight dynamics. But, why practical problems, such as those related to space flight dynamics, should

---

M. Guzzo (✉)

Dipartimento di Matematica Pura ed Applicata, Università degli Studi di Padova, Via Trieste, 63-35121, Padova, US

e-mail: guzzo@math.unipd.it

be concerned with these dynamical systems theories? A theoretical formulation of a practical problem could be the following one: given two points  $A$  and  $B$  of the phase-space, one would find an orbit  $x(t)$  with initial condition  $x(0)$  in a small neighbourhood of  $A$  and  $x(T)$  in a small neighbourhood of  $B$  at some time  $T$ . In the hypothesis that such an orbit is found, it is usually affected by chaos, i.e. very small changes in the initial condition  $x(0)$  can result in big changes in the complete orbit  $x(t)$ . In addition, in presence of chaos, the orbits display topological and statistical complexities, and the transfer in the phase-space is often called (chaotic) diffusion. Numerical integrations of chaotic diffusion are intrinsically affected by large numerical errors, which become relevant on a finite (and usually short) time called Lyapunov time. The analysis of the orbits on times of the order of the Lyapunov times requires a detailed dynamical analysis of the phase-space structure of the systems. In the last decades many numerical indicators, based essentially on the Lyapunov characteristic exponents (such as the so called Fast Lyapunov Indicators, introduced in [4]) or on the Fourier analysis (such as frequency analysis [14, 15]) have been successfully used to detect the phase-space structure of non-integrable systems (see, for example, [5]).

The peculiarity of chaos related to the existence of many different orbits with very close initial conditions on the one hand is clearly a problem for numerical integrations, on the other hand it provides the opportunity of constructing orbits with behave, in some sense, as one wishes, with very small corrections to a reference orbit. The branch of dynamical systems which studies the behavior of chaotic orbits under small corrections is known as shadowing theory, and it is motivated by the Anosov–Bowen theorem.

The problems which I have discussed above are related to the existence of peculiar structures in the phase-space called stable and unstable manifolds. Stable and unstable manifolds are defined (see Section 2) as the sets of points whose orbits are asymptotic in the past or in the future respectively to an hyperbolic invariant structure of the phase-space, such as an hyperbolic fixed point, periodic orbit or invariant torus. Specifically, having in mind the problem of finding transfer orbits between points  $A$  and  $B$  of the phase-space, when the points  $A$  and  $B$  belong to different hyperbolic invariant sets which we denote by  $\mathcal{A}$ ,  $\mathcal{B}$  and the unstable manifold  $W^u$  of  $\mathcal{A}$  intersects the stable manifold  $W^s$  of  $\mathcal{B}$ , there exists the possibility of such transfer orbits between a neighbourhood of  $\mathcal{A}$  and a neighbourhood of  $\mathcal{B}$ . If the intersection of these manifolds is transverse, the possibility of transfer orbits is coupled to complicate dynamics, usually called “chaotic” dynamics. In this paper I describe the structure of stable/unstable manifolds for a class of dynamical systems which have been often used as the prototype of conservative systems, that is the symplectic maps. In Section 2 we analyze the structure of these manifolds in one of the simplest examples in which the structure is already complex, i.e. the homoclinic tangle of hyperbolic saddle points of the standard map and of more general two dimensional dynamical systems. In Section 3 we describe how diffusion can be supported by the heteroclinic tangle related to different periodic orbits. In Section 4 we describe some higher dimensional examples related to Arnold diffusion.

## 2 The Homoclinic Tangle of Hyperbolic Saddle Points

The paradigm of chaotic dynamics in conservative systems is represented by the so-called standard map  $(I, \varphi) \mapsto (I', \varphi')$  defined by:

$$\begin{aligned}\varphi' &= \varphi + I \\ I' &= I + \varepsilon \sin(\varphi + 1),\end{aligned}\tag{1}$$

where  $I \in \mathbb{R}$  is an action variable,  $\varphi \in \mathbb{S}^1$  is an angle and  $\varepsilon \in \mathbb{R}$  is a parameter. For  $\varepsilon = 0$  the standard map is integrable, i.e. the action  $I$  is constant while the angle  $\varphi$  rotates with angular velocity  $I$ .

Instead, for  $\varepsilon \neq 0$  the phase-portraits of the map (represented in Fig. 1) show the existence of invariant curves, as well as of two dimensional regions where motions seem to be spread, and certainly not organized in invariant curves. This peculiar structure of the phase-plane qualifies the standard map as a non integrable system.

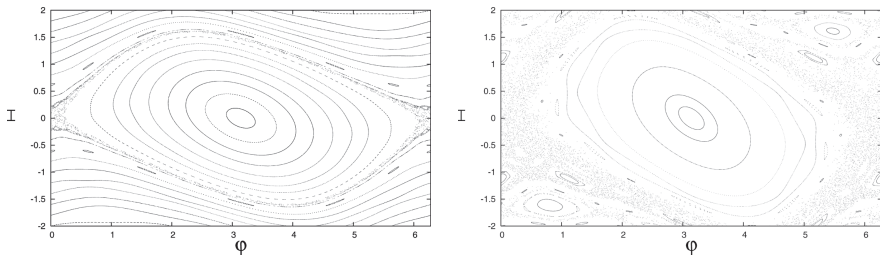


**Fig. 1** Phase portraits of the standard map for  $\varepsilon = 0.6$  (left panel) and  $\varepsilon = 1$  (right panel). In both cases the phase-plane contains a mixture of invariant curves and two dimensional regions where motions seem to spread uniformly. This peculiar structure of the phase-plane qualifies the standard map as a non integrable system

We remark also the presence of two fixed points  $(I, \varphi) = (0, 0), (0, \pm \pi)$ , and  $(0, 0)$  is an hyperbolic saddle point.

Two dimensional symplectic maps similar to the standard map can be obtained as Poincaré sections of higher dimensional continuous dynamical systems. An interesting example is provided by a simplified model of the spin-orbit rotations of oblate satellites, which is described in Fig. 2.

Because the fixed point  $x_* = (I_*, \varphi_*) = (0, 0)$  is a saddle point, one can apply the so called stable (unstable) manifold theorem (see [13]) to prove that the sets:

$$W^s = \{x: \lim_{t \rightarrow \infty} \psi^t(x) = x_*\}, \quad W^u = \{x: \lim_{t \rightarrow \infty} \psi^{-t}(x) = x_*\}\tag{2}$$

are smooth curves, locally tangent in  $x_*$  to the eigenvectors of the Jacobian matrix of  $\psi: \frac{\partial \psi}{\partial x}(x_*)$ . The manifold  $W^s$  is called stable manifold of  $x_*$ ,  $W^u$  is called unstable manifold of  $x_*$ .

In every two-dimensional dynamical system defined by a smooth map  $\psi: M \rightarrow M$  ( $M$  denotes the two-dimensional phase-space) with a saddle fixed point  $x_*$  the

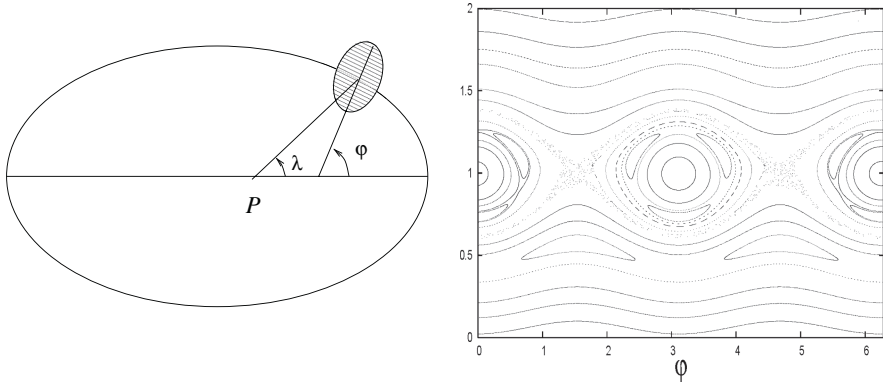


**Fig. 2** *Left* panel: a tri-axial satellite, whose center of mass moves on a Keplerian orbit, is constrained to rotate in the plane  $x,y$  around an axis of inertia. The equation of motion for the libration angle  $\varphi$  is:  $\ddot{\varphi} = -\frac{3}{2}\Omega^2\left(\frac{a}{|r|}\right)^3\frac{I_2-I_1}{I_3}\sin(2(\varphi-\lambda))$ , where  $\lambda, a, r$  denote the true longitude, the semi-major axis and the distance from the center of mass to the central body;  $\Omega$  denotes the Keplerian frequency of motion and  $I_1, I_2, I_3$  are the principal moments of inertia. *Right* panel: phase portrait of the Poincaré map  $(\varphi, I) = (\varphi(0), \dot{\varphi}(0)) \mapsto (\varphi', I') = (\varphi(T), \dot{\varphi}(T))$ , with  $T = 2\pi/\Omega$ . The eccentricity of the orbit is 0.02 and  $\frac{3}{2}\Omega^2\frac{I_2-I_1}{I_3} = 0.075$ . The phase-plane structure is qualitatively similar to the phase-plane structure of the standard map shown in Fig. 1: the phase-plane contains a mixture of invariant curves and two dimensional regions where motions seem to spread uniformly. This peculiar structure of the phase-plane qualifies this dynamical system as a non integrable system

stable and unstable manifolds of  $x_*$  are curves. From the definition it is clear that the knowledge of the unstable manifold  $W^u$  provides knowledge about how the orbits with initial conditions in a small neighbourhood of  $x_*$  “go away” from  $x_*$ , while the knowledge of the stable manifold  $W^s$  provides knowledge about how the orbits of the phase-space approach asymptotically  $x_*$ .

In the two-dimensional systems with a first integral the stable and unstable manifolds are contained in the level set of the first integral containing the fixed point. Therefore, they do not have a complicate topology. To produce a complicate topology we need different hypotheses. An hypothesis which is sufficient to prove the existence of a complicate structure for the stable and unstable manifolds due to Poincaré [18] is related to the existence of a so-called homoclinic point  $x_0$ , that is a point of transverse intersection of  $W^s, W^u$ . In such a case, one shows that:

- each point of the orbit of the homoclinic point  $x_0$ :

$$x_t = \psi^t(x_0) \quad t \in \mathbb{Z}$$

is an homoclinic point, i.e.  $W^s$  intersects  $W^u$  transversely at  $x_t$ .

- As a consequence, the unstable manifold cuts the stable manifold transversely infinite times forming typical lobes, as it is shown in Fig. 3.

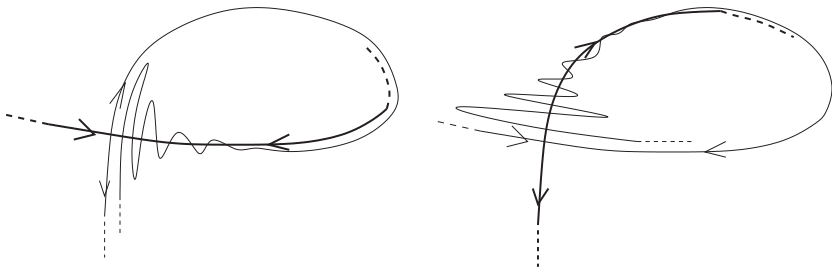


**Fig. 3** Examples of structure of stable and unstable manifolds of a saddle fixed point of a two dimensional system, with the hypothesis of existence of homoclinic points. *Left* panel: the unstable manifold of  $x_*$  cuts the stable manifold (represented by the bold curve) transversely forming typical lobes. *Right* panel: the stable manifold cuts the unstable manifold (represented by the bold curve) transversely forming typical lobes

- Approaching the fixed point the base of each lobe becomes smaller and the height becomes bigger, because near the fixed point there is contraction along the stable direction and expansion along the unstable one.
- Suitably close to  $x_*$ , the lobes of the unstable manifold are so long that they are forced to intersect the stable manifold in points  $x', x''$  which are not in the orbit of  $x_0$ . Also the orbits of these points contain only homoclinic points (Fig. 4).

All these properties demonstrate that in the hypothesis of existence of at least an homoclinic point the structure of the stable and unstable manifolds is indeed very complicate, and is commonly called homoclinic tangle. We remark that because  $W^u$  is the set of all the points whose orbit “comes from the fixed point  $x_*$ ” (for  $t \rightarrow -\infty$ ) and  $W^s$  is the set of all the points whose orbit “goes to the fixed point  $x_*$ ” (for  $t \rightarrow +\infty$ ), the homoclinic points are the points whose orbit “comes from and goes to the fixed point  $x_*$ ”. Therefore, the complexity of the structure of the homoclinic tangle reflects the complexity of the dynamics related to the saddle point. A precise way of representing the complex dynamics in homoclinic tangles uses the conjugation of the map  $\psi$  to special maps called “horseshoe” maps (see [20]).

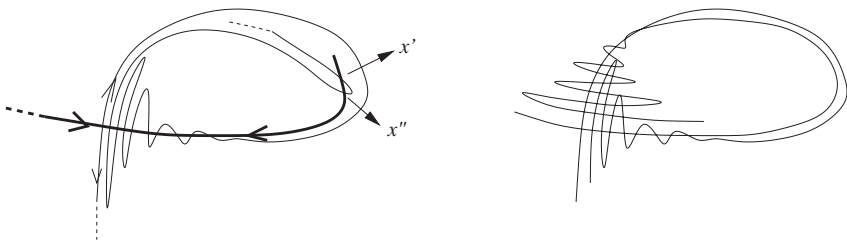


**Fig. 4** Examples of structure of stable and unstable manifolds of a saddle fixed point of a two dimensional system, with the hypothesis of existence of homoclinic points. *Left* panel: the homoclinic points  $x'$  and  $x''$  are not in the same homoclinic orbit. *Right* panel: homoclinic tangle near the fixed point

In general, the analytic computation of the stable and unstable manifolds, as well as the analytic determination of homoclinic points, is not straightforward. In some perturbative contexts, analytical approximations can be obtained by means of the so called Poincaré–Melnikov integrals.

Instead, the numerical localization of  $W^s$ ,  $W^u$ , at least in the described case of two dimensional maps, can be obtained by numerically propagating a set of initial conditions chosen in a small neighborhood of the saddle point. In such a way, one directly constructs a neighborhood of a finite piece of the unstable manifold, while for the stable manifold one repeats the construction for the inverse map. This method gives very good results for two dimensional maps because the neighborhoods of the fixed points are two dimensional and can be propagated with reasonable CPU times. A more sophisticated method is described in [19]. In Fig. 5 we show the numerical computation of the stable and unstable manifolds of the fixed point (0,0) of the standard map: from the figures we appreciate the topological complexity of the homoclinic tangle.

### 3 From Chaos to Diffusion in two Dimensional Symplectic Maps

In the previous section we have described the structures which support chaotic motions in two-dimensional symplectic maps. However, the existence of chaotic motions does not mean that the system is characterized by macroscopic instability. For example, the region interested by chaotic motions could be localized in a small region of the phase-space. To better represent this situation, instead of the usual standard map (1), we consider a slightly different map defined by:

$$\begin{aligned}\varphi' &= \varphi + I \\ I' &= I + \varepsilon \frac{\sin \varphi'}{(\cos \varphi' + 1.1)^2}.\end{aligned}\tag{3}$$

The map (3) is more suitable than (1) to represent generic quasi-integrable maps, because the Fourier expansion of the perturbation:

$$f(\varphi') = \varepsilon \frac{\sin \varphi'}{(\cos \varphi' + 1.1)^2}\tag{4}$$

contains an infinite number of harmonics. The advantage of using maps of the form (3) has been explained in several papers [5, 7, 8, 6, 9]. We now consider the phase portraits of the map reported in Fig. 6: for  $\varepsilon = 0.002$  (left panel) the phase-space contains regions characterized by chaotic motions (such as those with action around the value  $I = 0.34$  and  $I = 0.36$ ) which are disconnected by invariant curves, acting as complete barriers to the diffusion of the action variable  $I$ . Therefore, there do not exist orbits which connect these different chaotic regions. The invariant curves which are complete barriers to the diffusion of the action variable are KAM curves,

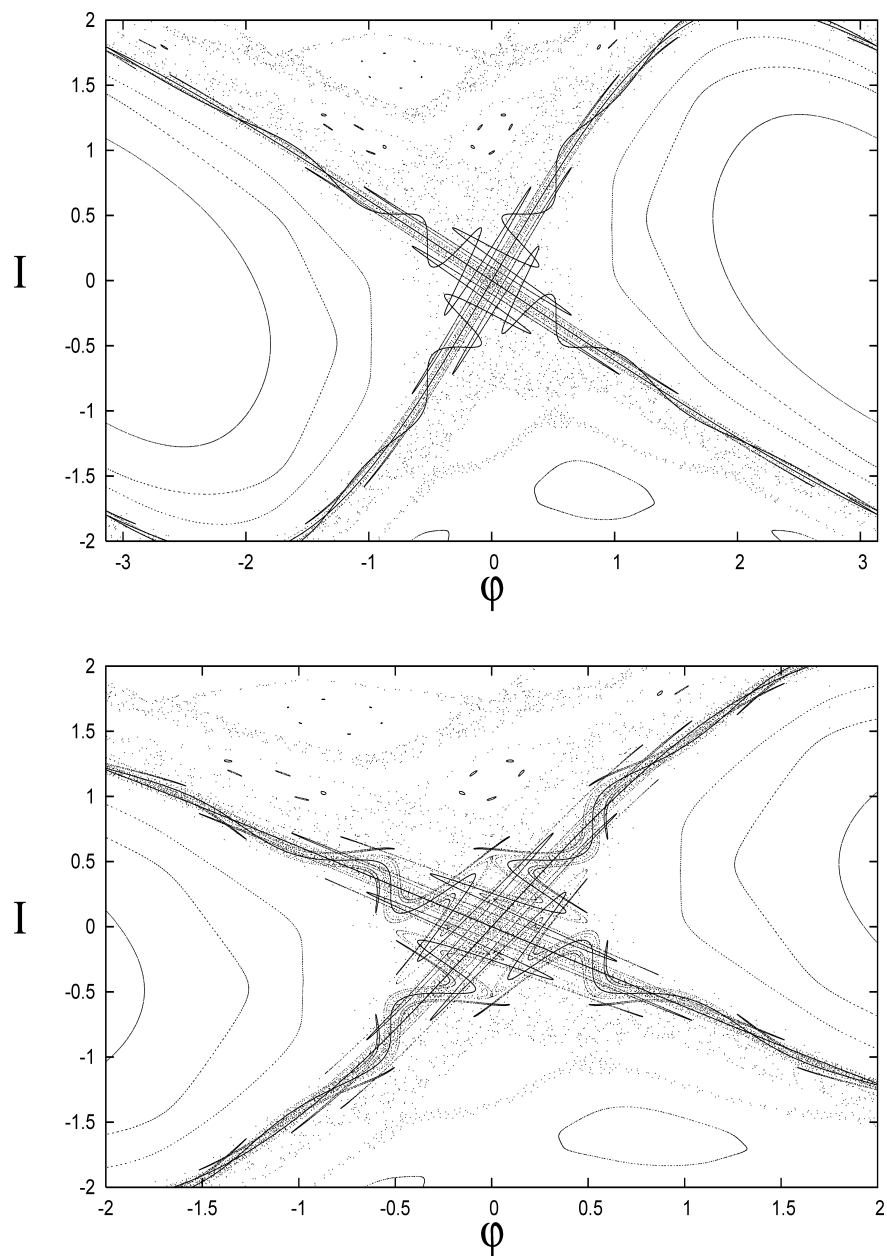


**Fig. 5** Numerical representation of finite pieces of the stable and unstable manifolds of the hyperbolic fixed point  $(0,0)$  of the standard map for  $\varepsilon = 1$ . On each panel the stable and unstable manifolds are plotted on the phase portrait of the map. The *top* panel represents a shorter piece of the manifold

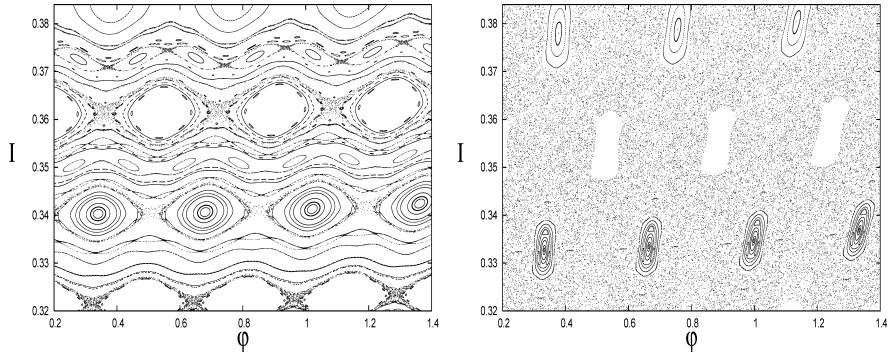


**Fig. 6** Phase portraits of the map (3) for  $\varepsilon = 0.002$  (left panel) and  $\varepsilon = 0.004$  (right panel). For the smallest value of  $\varepsilon$  we see that there exist invariant curves which act as topological barriers to the diffusion of the action  $I$ . For the largest value of  $\varepsilon$  the absence of invariant curves means that, in principle, an orbit can diffuse through all the action values

whose existence can be established by the KAM theorem (Kolmogorov [10], Arnold [2], Moser [17]). The KAM theorem proves the existence of the KAM invariant curves if the value of the perturbing parameter  $\varepsilon$  is suitably small. Instead, for higher values of  $\varepsilon$  the KAM curves typically are destroyed and replaced by the so called cantori, which are discontinuous Aubry–Mather invariant sets, and therefore the action variables can diffuse through their holes. In Fig. 6, right panel, we represent a the phase portrait of the map (3) for  $\varepsilon = 0.004$ : for such an higher value of the perturbing parameter we do not find KAM curves on the phase-portrait. The absence of the topological barriers represented by the KAM invariant curves allow the chaotic orbits to possibly diffuse through all the action values.

The possibility of an orbit of diffusing through all the action values does not mean that there exist orbits which effectively diffuse. Up to now, there does not exist a rigorous explanation of global diffusion in generic quasi-integrable systems, while there exist heuristic criteria. One of the most popular heuristic criteria for establishing the existence of global diffusion is the so called Chirikov criterion [3] of overlapping resonances. The idea behind Chirikov criterion is that global diffusion exists when the hyperbolic regions related to the hyperbolic periodic orbits of different resonances “overlap”. A rigorous way of defining the overlapping of nearby resonances uses the stable and unstable manifolds of these periodic orbits. Precisely, a periodic orbit of period  $k$  for a map  $\psi: M \rightarrow M$  is defined by a sequence  $x_j \in M$ ,  $j = 0, \dots, k-1$  such that  $\psi(x_j + k) = \psi(x_j)$  for any  $j$ . In particular, any point  $x_j$  is a fixed point of the map  $\psi^k$ . We now consider the periodic orbits of initial conditions  $x_0$  such that  $x_0$  is a saddle fixed point of  $\psi^k$ . One can therefore define stable and unstable manifolds for  $x_0$  as in the case of fixed points, and look for homoclinic intersections, producing the homoclinic tangle and chaotic motions. But now one can do more and can look for the transverse intersections between the stable/unstable manifolds of the different fixed points of the map  $\psi^k$  which correspond to different periodic orbits (or fixed points) of the map  $\psi$ .



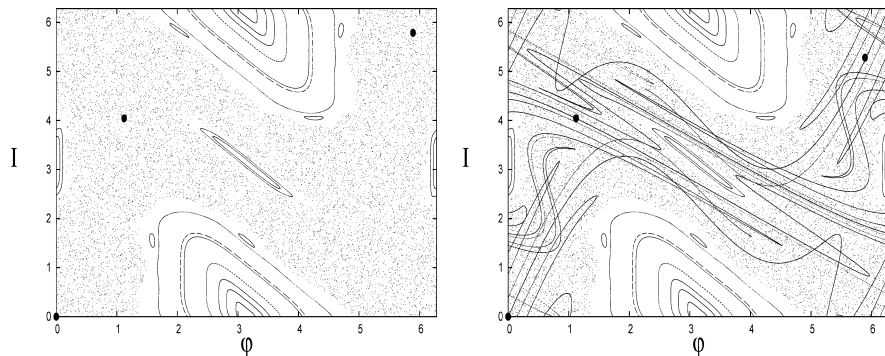


**Fig. 7** Numerical computation of heteroclinic points among the unstable manifold of a saddle fixed point and the stable manifold of a periodic orbit of period  $k = 2$  of the standard map for  $\varepsilon = 2$ . *Left panel*: phase-portrait of  $\psi^2$ , where  $\psi$  denotes the standard map (1). The bullet denotes the initial condition of an hyperbolic periodic orbit of period  $k = 2$ . *Right panel*: on the phase-portrait we report the computation of a finite piece of the unstable manifold of  $(0,0)$  and the stable manifold of the hyperbolic periodic orbit. We can appreciate the presence of many heteroclinic intersections

Let us consider the following example: let  $\psi$  be the standard map (1) with  $\varepsilon = 2$  and let us consider the periodic orbits of period  $k = 2$ . The map  $\psi^2$  has  $(0,0)$  as saddle fixed point, but also a saddle fixed point  $x_0 = (\varphi_0, I_0)$  which corresponds to an hyperbolic periodic orbit of the standard map of period 2 (see Fig. 7, left panel). The numerical computation of the phase portrait shows that there are not invariant KAM curves which act as topological barriers to the diffusion of the action variable in the interval  $[0, I_0]$ . To show that diffusion indeed occurs in this interval, we use the mechanism provided by the existence of transverse intersections among the stable manifold of one periodic orbit and the unstable manifold of the fixed point  $(0,0)$ . Such transverse intersection points are called heteroclinic points, and they are used since decades to explain global diffusion in the phase-space. Establishing the existence of heteroclinic points rigorously is even more difficult than for homoclinic points. Instead, numerical methods apply without additional difficulties. In Fig. 7, right panel, we report the numerical computation of the unstable manifold of  $(0,0)$  and the stable manifold of  $x_0$ : the existence of transverse intersections is evident. Because of the existence of heteroclinic points one easily finds initial conditions which chaotically diffuse from a neighbourhood of the fixed points  $(0,0)$  to a neighborhood of the periodic orbit of initial condition  $x_0$ .

#### 4 Higher Dimensional Systems: from Arnold's Model to Four Dimensional Maps

The general mechanisms which can produce drift and diffusion in the phase-space of higher dimensional systems is an interesting, and in general open, problem.

The problem becomes more difficult when the system is close to an integrable one. Interesting examples of chaos and diffusion in a three-body problem using stable/unstable manifolds is described in [16].

Many diffusive phenomena in higher dimensional systems are called Arnold diffusion, because they are more or less inspired by the pioneering example proposed by Arnold [1]. Arnold's example is defined by the Hamiltonian system:

$$H = \frac{I_1^2}{2} + \frac{I_2^2}{2} + \varepsilon \cos \varphi_1 + \varepsilon \mu (\cos \varphi_1 - 1)(\sin \varphi_2 + \sin t), \quad (5)$$

where  $\varphi_1, \varphi_2 \in \mathbb{S}^1$ ,  $I_1, I_2 \in \mathbb{R}$ , and  $\varepsilon, \mu$  are parameters. The Hamilton equations of (5) are:

$$\begin{aligned} \dot{\varphi}_1 &= I_1 \\ \dot{\varphi}_2 &= I_2 \\ \dot{I}_1 &= \varepsilon \sin \varphi_1 + \varepsilon \mu \sin \varphi_1 (\sin \varphi_2 + \sin t) \\ \dot{I}_2 &= -\varepsilon \mu (\cos \varphi_1 - 1) \cos \varphi_2. \end{aligned} \quad (6)$$

The system depends on two small parameters  $\varepsilon$  and  $\mu$ . For  $\varepsilon = 0$  the system has only three dimensional invariant tori (considering  $t$  as a periodic variable with equation  $\dot{t} = 1$ ) defined by the constant value of the actions  $I_1, I_2$ , and the motions on these tori are quasi-periodic with three frequencies:

$$\dot{\varphi}_1 = I_1 \quad \dot{\varphi}_2 = I_2 \quad \dot{t} = 1. \quad (7)$$

For  $\varepsilon, \mu \neq 0$  the system becomes non integrable, and understanding its dynamics is not trivial. Specifically, for suitably small  $\varepsilon$  the KAM theorem (in its hysoenergetic formulation) applies to Hamiltonian (5), establishing the existence of a large volume set of invariant tori in the phase-space. However, at variance with the case of two dimensional maps, where KAM curves divided the phase-space acting as complete barriers for diffusion, in such a five dimensional system the three dimensional invariant tori do not divide the phase-space, and diffusion of orbits among the invariant tori is in principle possible.

To prove the existence of diffusion, Arnold considered the special resonance:  $\dot{\varphi}_1 = 0$ , which contains an invariant manifold  $\Lambda$  defined by  $I_1 = 0, \varphi_1 = 0$ . The invariant manifold  $\Lambda$  is fibered by the invariant two dimensional tori:

$$I_1 = 0 \quad \varphi_1 = 0 \quad \dot{\varphi}_2 = I_2(0) \quad \dot{t} = 1, \quad (8)$$

which are hyperbolic if  $\mu$  is suitably small. In fact, for  $\mu = 0$  the Hamiltonian of the system is:

$$H = \frac{I_1^2}{2} + \varepsilon \cos \varphi_1 + \frac{I_2^2}{2},$$

which is the Hamiltonian of a pendulum and a rotator. In this case, the stable and unstable manifolds of each invariant torus (8) are the separatrices of the pendulum.

As a consequence, for  $\mu = 0$ , the invariant manifold  $\Lambda$  is hyperbolic. By general hyperbolic theory the manifold  $\Lambda$  remains hyperbolic also for suitably small  $\mu \neq 0$ .

We remark that for  $\mu = 0$  the action  $I_2$  is a first integral of the system, while for  $\mu \neq 0$  it is a first integral only for the restriction of the map to the invariant manifold  $\Lambda$ . Therefore, there is not diffusion of the action  $I_2$  on  $\Lambda$ , but as soon as  $\varepsilon, \mu \neq 0$  the action  $I_2$  can diffuse in any small neighbourhood of  $\Lambda$ . To prove that this diffusion indeed exists, Arnold proved that the unstable manifolds of hyperbolic tori of  $\Lambda$  intersect transversely the stable manifolds of close hyperbolic tori, thus providing the mechanism for initial conditions in the neighbourhood of  $\Lambda$  to diffuse through these manifolds. This kind of diffusion is called Arnold diffusion.

Though the results on the Arnold's model have not been generalized to generic quasi-integrable systems, the ideas contained in Arnold's work have inspired in the last decades the studies of diffusion in higher dimensional systems. Below, we describe recent numerical studies of slow diffusion in four dimensional quasi-integrable systems inspired by Arnold's model of diffusion. [5, 7, 11, 8, 6, 9].

In many papers in collaboration with Froeschlé and Lega [5, 7, 8, 6, 9, 12] we considered specific quasi-integrable systems which are more generic than Arnold's model. Specifically, we considered two coupled twist maps as follows:

$$\begin{aligned} \varphi'_1 &= \varphi_1 + I_1, \varphi'_2 = \varphi_2 + I_2 \\ I'_1 &= I_1 - \varepsilon \frac{\partial f}{\partial \varphi_1}(\varphi'_1, \varphi'_2), I'_2 = I_2 - \varepsilon \frac{\partial f}{\partial \varphi_2}(\varphi'_1, \varphi'_2) \end{aligned} \quad (9)$$

where  $\varepsilon$  is a small parameter and the perturbation  $f$  is:

$$f = \frac{1}{\cos(\varphi_1) + \cos(\varphi_2) + c}$$

with  $c > 2$ . This specific choice of the perturbation has been done because the Fourier expansion of  $f$  contains an infinite number of harmonics, and the exponential decay of the harmonics is determined by the choice of the constant  $c$ .

If  $\varepsilon = 0$  the map (9) is integrable: the actions of this system are constants of motion and the angles rotate at constant angular velocity. Because it is not possible to represent the orbits of (9) in the complete four dimensional phase-space, it is convenient to represent them on a two dimensional surface such as:

$$S = \{(I_1, I_2, \varphi_1, \varphi_2): (\varphi_1, \varphi_2) = (0, 0)\}.$$

For  $\varepsilon = 0$ , any orbit with initial condition  $x$  on  $S$  is on an invariant torus. Therefore, the orbit does not return on  $S$  if the ratio of the frequencies is irrational, or it returns exactly on  $S$  on the point  $x$  if the ratio of the frequencies is rational. Therefore, each orbit with initial conditions on  $S$  can be symbolically represented by a dot on  $S$ .

If  $\varepsilon \neq 0$  the system is not integrable and the actions are not constants of motion, but if  $\varepsilon$  is sufficiently small, the phase-space is filled by a large volume of two dimensional KAM tori. Anyone of these tori intersects transversely  $S$  only on one

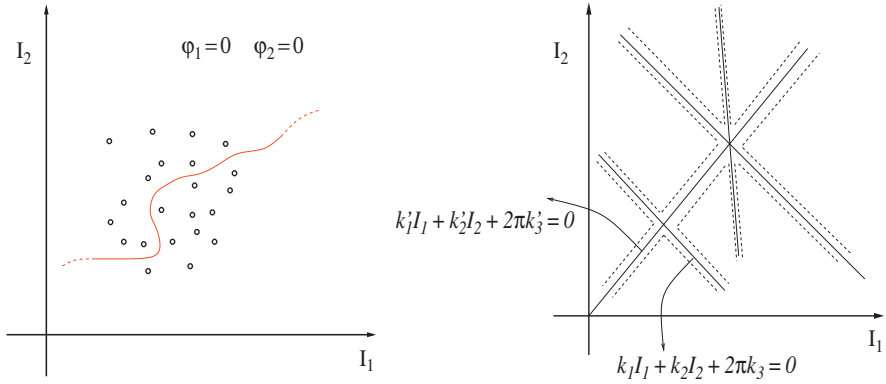


**Fig. 8** *Left* panel: the KAM tori do not trap motions in the four dimensional space. *Right* panel: the KAM tori are outside the neighborhood of the resonances defined by the Diophantine condition (12)

point (see [7]), and therefore each invariant torus is symbolically represented by a point on  $S$ . Therefore, the surface  $S$  contains many points representing two dimensional invariant tori, which however do not trap motions in the four dimensional phase-space. There is therefore the possibility of diffusion among these invariant tori even for very small  $\varepsilon \neq 0$  (see Fig. 8 for a symbolic representation of possible diffusion paths).

Diffusion, as far as we know, needs hyperbolic structures, which are related to the resonances of the system, therefore we need a method to identify the hyperbolic structures of the map. We first recall the definition of the resonances for the map (9). Any linear combination of the angles  $k_1\varphi_1 + k_2\varphi_2$ , with  $k_1, k_2 \in \mathbb{Z}$ , is resonant if there exists  $k_3 \in \mathbb{Z}$  such that:

$$k_1\varphi'_1 + k_2\varphi'_2 = (k_1\varphi_1 + k_2\varphi_2) + (k_1I_1 + k_2I_2) = (k_1\varphi_1 + k_2\varphi_2) + 2\pi k_3, \quad (10)$$

i.e. if:

$$k_1 I_1 + k_2 I_2 - 2\pi k_3 = 0. \quad (11)$$

From KAM theorem we know that invariant tori are located far from a suitable neighbourhood of all these resonances (see Fig. 8). In fact, a KAM torus exists near the values  $(I_1, I_2)$  satisfying a non-resonance Diophantine condition of the form:

$$|k_1 I_1 + k_2 I_2 - 2\pi k_3| \geq \frac{\mathcal{O}(\sqrt{\varepsilon})}{|(k_1, k_2, k_3)|^\tau}, \quad \forall (k_1, k_2, k_3) \in \mathbb{Z}^3 \setminus (0, 0, 0), \tau > 2. \quad (12)$$

The complement of the set of invariant tori, which is in the neighbourhood of the resonances, is called Arnold web, and contains the hyperbolic structures which possibly support chaotic diffusion. An efficient way of detecting numerically the Arnold web of a system is provided by the so called Fast Lyapunov Indicator, first defined

in [4]. For a generic map  $\psi: M \rightarrow M$  the Fast Lyapunov Indicator  $FLI(x, v, T)$  is a function which depends on a point  $x \in M$ , on a tangent vector  $v \in \mathbb{R}^n = T_x M$ , and on a positive time  $T$  as follows:

$$FLI(x, v, T) = \log \left\| \frac{\partial \psi^T}{\partial x}(x) v \right\|. \quad (13)$$

For a fixed vector  $v$  and suitably long time  $T$  the computation of the function  $FLI(x, v, T)$  on the surface  $S$  provides a precise detection of the Arnold web and of the hyperbolic structures of the system, as it is explained in detail in [5, 7]. Here, we report the results of the computation of the FLI for the map (9) on the surface  $S$ . For any point  $x$  on a grid of  $S$  we computed the Fast Lyapunov Indicator, and represented it with a color scale. Precisely,

- the points with the higher values of the FLI (which corresponds to white in the color scale used to represent the value of the indicator) denote motions on hyperbolic structures within the resonances of the system;
- the points with an intermediate value of the FLI (which corresponds to intermediate gray in the color scale used to represent the value of the indicator) are regular motions (including KAM tori);
- the points with lower value of the FLI (which corresponds to black or dark gray in the color scale used to represent the value of the indicator) are regular motions (including resonant tori).

Therefore, the color representation of the FLI on  $S$  allows one to clearly identify the KAM tori, the resonant tori, as well as the hyperbolic structures which possibly support diffusion in the phase-space. The result of the computation is reported in Fig. 9. For  $\varepsilon = 0.6$  (left panel) there is a prevalence of KAM tori in the phase-space,

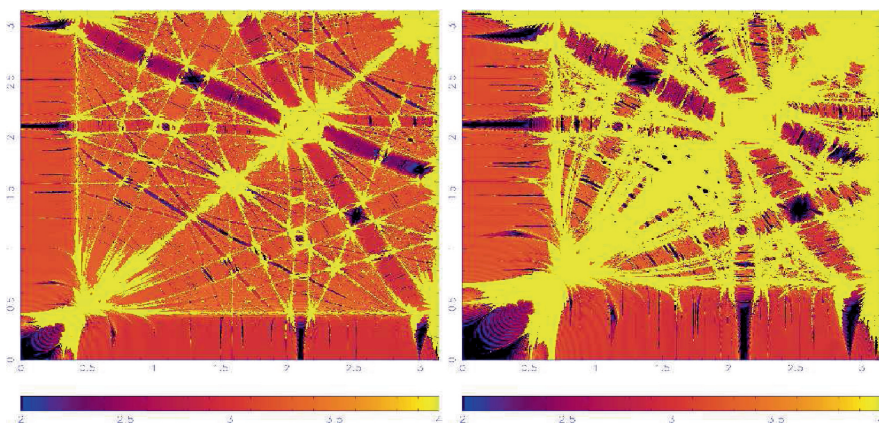


**Fig. 9** Computation of the Arnold web on the section  $S$  using a color representation of the FLI. *Left panel:*  $\varepsilon = 0.6$ ,  $c = 4$ . *Right panel:*  $\varepsilon = 1.6$ ,  $c = 4$ .

and the hyperbolic structures are organized as a web of resonances, as predicted by the KAM theorem. Chaotic diffusion can occur only on this network of hyperbolic structures. Instead, for the higher value  $\varepsilon = 1.6$  there is a prevalence of hyperbolic motions. In such a case, the hyperbolic structures are not organized in a web, we are not in a regime described by the KAM theorem, and chaotic diffusion can occur practically in any direction.

In [11, 8] we have shown how initial conditions in the hyperbolic manifolds diffuse in the Arnold web. We have chosen initial conditions in the region of the hyperbolic motions and then we computed numerically their orbits up to the very long  $10^{11}$  iterations. The results are reported in Fig. 10: on the section  $S$ , represented

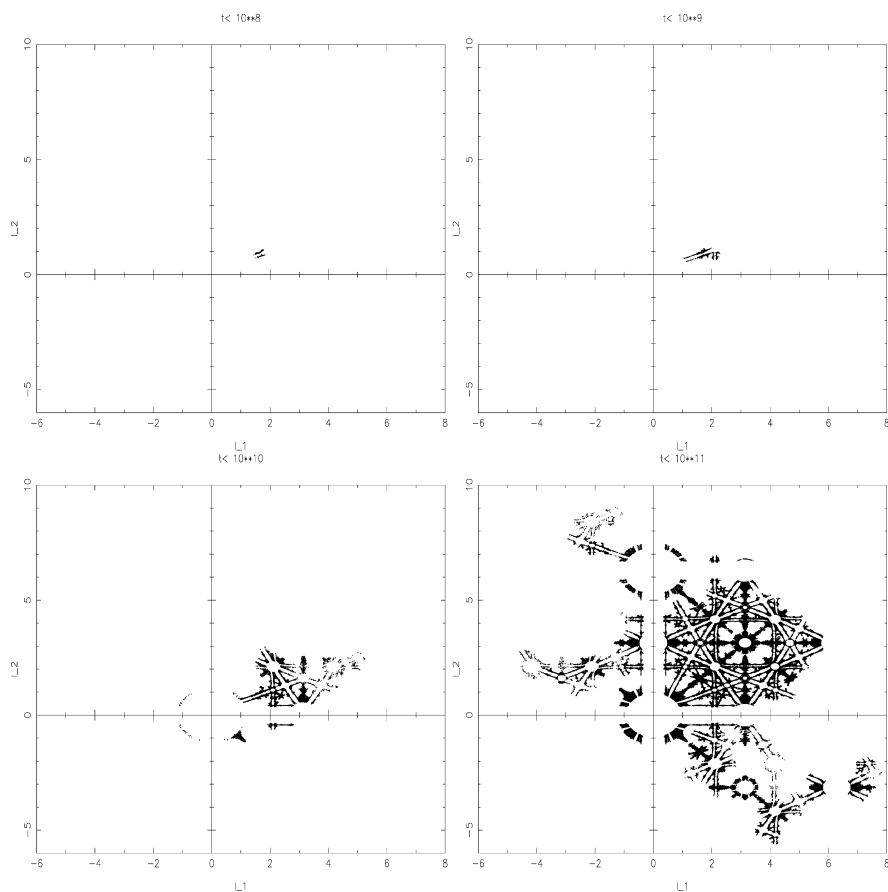


**Fig. 10** Evolution on section  $S$  (black dots) of 20 orbits for the map (9) with hyperbolic initial conditions near  $(I_1, I_2) = (1.71, 0.81)$  on a time  $t < 10^8$  iterations (top left),  $t < 10^9$  iterations (top right),  $t < 10^{10}$  iterations (bottom left),  $t < 10^{11}$  iterations (bottom right) for  $\varepsilon = 0.6$ . The orbits fill a macroscopic region of the action plane whose structure is that of the Arnold web

by the action plane, we plotted as black dots all points of the orbits which have returned after some time near the section  $S$ . Because computed orbits are discrete we represented the points which enter the neighbourhood of  $S$  defined by  $|\varphi_1|, |\varphi_2| \leq 0.005$ , (reducing the tolerance 0.005 reduces only the number of points on the section, but does not change their diffusion properties). In such a way we represent the chaotic diffusion for orbits with initial conditions in a neighborhood of  $S$ . It happens that the orbits fill a macroscopic region of the action plane whose structure is that of the Arnold web. The possibility of visiting all possible resonances is necessarily limited by finite computational times.

## References

1. Arnold V.I. (1964), Instability of dynamical systems with several degrees of freedom, *Sov. Math. Dokl.*, **6**, 581–585.
2. Arnold V.I. (1963a), Proof of a theorem by A.N. Kolmogorov on the invariance of quasi-periodic motions under small perturbations of the Hamiltonian. *Russ. Math. Surv.*, **18**, 9.
3. Chirikov, B.V. (1979), An universal instability of many dimensional oscillator system. *Phys. Reports*, **52**, 265.
4. Froeschlé C., Lega E. and Gonczi R. (1997), Fast Lyapunov indicators. Application to asteroidal motion. *Celest. Mech. and Dynam. Astron.*, **67**, 41–62.
5. Froeschlé C., Guzzo M. and Lega E. (2000), Graphical Evolution of the Arnold Web: From Order to Chaos, *Science*, **289**, n. 5487.
6. Froeschlé C., Guzzo M. and Lega E. (2005), Local and global diffusion along resonant lines in discrete quasi-integrable dynamical systems, *Celest. Mech. and Dynam. Astron.*, **92**, n. 1-3, 243-255.
7. Guzzo M., Lega E. and Froeschlé C. (2002), On the numerical detection of the effective stability of chaotic motions in quasi-integrable systems, *Physica D*, **163**, n. 1-2, 1-25.
8. Guzzo M., Lega E. and Froeschlé C. (2005), First Numerical Evidence of Arnold diffusion in quasi-integrable systems, *DCDS B*, **5**, n. 3.
9. Guzzo M., Lega E. and Froeschlé C. (2006), Diffusion and stability in perturbed non-convex integrable systems. *Nonlinearity*, **19**, 1049–1067.
10. Kolmogorov, A.N. (1954), On the conservation of conditionally periodic motions under small perturbation of the hamiltonian, *Dokl. Akad. Nauk. SSSR*, **98**, 524.
11. Lega E., Guzzo M. and Froeschlé C. (2003), Detection of Arnold diffusion in Hamiltonian systems, *Physica D*, **182**, 179–187.
12. Lega E., Froeschlé C. and Guzzo M. (2007), Diffusion in Hamiltonian quasi-integrable systems.” In *Lecture Notes in Physics*, “Topics in gravitational dynamics”, Benest, Froeschlé, Lega eds., Springer.
13. Hirsch M.W., Pugh C.C. and Shub M. (1977), Invariant Manifolds. Lecture Notes in Mathematics, **583**. Springer-Verlag, Berlin-New York.
14. Laskar, J. (1989), A numerical experiment on the chaotic behaviour of the solar system, *Nature*, **338**, 237–238.
15. Laskar, J. (1990), The chaotic motion of the solar system - A numerical estimate of the size of the chaotic zones. *Icarus* **88**, 266–291.
16. Llibre, J. Sim, C. (1980), Some homoclinic phenomena in the three-body problem. *J. Diff. Eq* **37**, no. 3, 444–465.
17. Moser J. (1958), On invariant curves of area-preserving maps of an annulus, *Comm. Pure Appl. Math.*, **11**, 81–114.

18. Poincaré H. (1892), *Les méthodes nouvelles de la mécanique celeste*, Gauthier–Villars, Paris.
19. Simo C. (1989), On the analytical and numerical approximation of invariant manifolds, in *Modern Methods in Celestial Mechanics*, D. Benest, Cl. Froeschlé eds, Editions Frontières, 285-329.
20. Smale S. (1967), Differentiable dynamical systems, *Bulletin of the American Mathematical Society*, **73**, 747-817.



Space Manifold Dynamics  
Novel Spaceways for Science and Exploration  
Perozzi, E.; Ferraz-Mello, S. (Eds.)  
2010, XV, 258 p., Hardcover  
ISBN: 978-1-4419-0347-1